Pergamon

Int. Comm. Heat Mass Transfer, Vol. 27, No. 7, pp. 893–902, 2000
Copyright © 2000 Elsevier Science Ltd
Printed in the USA. All rights reserved
0735-1933/00/$–see front matter

PII: S0735-1933(00)00169-X

DIFFUSION OF BINARY MIXTURES IN MICROPOROUS MATERIALS: OVERSHOOT AND ROLL-UP PHENOMENA

R. Krishna
Department of Chemical Engineering, University of Amsterdam
Nieuwe Achtergracht 166, 1018 WV Amsterdam, The Netherlands
(Fax: +31 20 5255604; email: krishna@its.chem.uva.nl)

(Communicated by J.P. Hartnett and W.J. Minkowycz)

ABSTRACT

Diffusion of mixtures in microporous materials such as zeolites is complicated by two important factors: (1) the diffusion phenomena is strongly dependent on the adsorbed species loadings, and (2) the diffusion of one component has a direct influence on the diffusion of the other component(s). In order to describe the diffusion process we adopt the Maxwell-Stefan formulation; this allows the prediction of mixture behaviour on the basis of information of the diffusion characteristics of the pure components in the mixture. Calculations are presented for several examples to illustrate the unusual characteristics of microporous diffusion. For uptake of a binary mixture into a spherical particle, for example, it is shown that the species with the higher mobility can "overshoot" its equilibrium loading during the transient uptake process. The slower-diffusing species experiences the "roll-up" phenomenon in its breakthrough characteristics through a packed bed adsorber filled with microporous particles. © 2000 Elsevier Science Ltd

Introduction

Microporous materials such as zeolites and carbon molecular sieves are widely used in the process industries [1 - 3]. Practical applications include: (1) production of nitrogen and oxygen from air by pressure swing adsorption using either carbon molecular sieve (CMS) or 5A zeolite, (2) hydrogen recovery from fuel gas using either activated carbon or zeolite, (3) separation of linear and branched hydrocarbons by diffusion selective sorption separation using 5A zeolite, and (4) landfill gas separation using CMS. In designing the adsorber, a proper description of the mass transfer process inside the microporous materials is essential. Diffusion in microporous materials is different from diffusion in other meso- or macro- porous media. In microporous media, the pores of the sorbent material are of the same order of magnitude as the molecular dimensions and usually of the order of a few nanometers and the diffusion process is strongly influenced by sorption.

A variety of models and techniques have been used to describe microporous diffusion, ranging from phenomenological models such as the Fick's law of diffusion [1,2] and the Maxwell-Stefan (MS) formulation [4 - 7] to Monte Carlo (MC) simulations [8,9] and Molecular Dynamics (MD) [10 - 14]. While MC and MD simulations are essential tools for gaining insights into diffusive transport within zeolites, such techniques are computationally too expensive to use in routine process simulations of say membrane transport or adsorber breakthrough. For process simulations, we still need to rely on phenomenological models, such as the Maxwell-Stefan formulation [4 - 7].

A recent paper by Ni and San [15] considers diffusion of a *single* species within a spherical microprous particle whereas in separation processes we have to reckon with *mixture* diffusion. The major objective of the present communication is to highlight some peculiar characteristics of *binary mixture* diffusion within microporous materials. We aim to show in mixture diffusion, coupling effects can lead to supra-equilibrium loadings of particular species within the particle. Before proceeding to mixture diffusion, we consider diffusion of a single component.

Single Component Diffusion Inside a Spherical Microporous Particle

The transient uptake is described by the following differential equation

$$\frac{\partial q_i}{\partial t} = -\frac{1}{\rho}\frac{1}{r^2}\frac{\partial}{\partial r}\left(r^2 N_i\right); \quad N_i = -\rho D_i \frac{\partial q_i}{\partial r} \tag{1}$$

where q_i is the species loading expressed as mol adsorbed per kg of microporous particle; N_i is the molar flux, expressed as mol/m^2/s; D_i is the Fick diffusivity; r is the radial distance coordinate; ρ is the density of the microporous particle expressed in kg/m^3. The Fick diffusivity of the diffusing species *i*, D_i, is strongly dependent on the loading q_I; this dependence is described by

$$D_i = Đ_i \Gamma_i; \quad \Gamma_i \equiv \frac{\partial \ln p_i}{\partial \ln q_i} = \frac{\partial \ln p_i}{\partial \ln \theta_i} \tag{2}$$

where θ_i the fractional occupancy is defined as $\theta_i = q_i/q_{i,sat}$; $q_{i,sat}$ is the saturation loading; $Đ_i$ is the Maxwell-Stefan diffusivity or "corrected" diffusivity. The Maxwell-Stefan diffusivity remains almost independent of the loading. The thermodynamic correction factor Γ_i can be calculated from the sorption isotherm. If the equilibrium is described by a Langmuir isotherm:

$$q_1 = \frac{q_{1,sat} b_1 P}{1 + b_1 P}; \quad \theta_1 = \frac{b_1 P}{1 + b_1 P} \tag{3}$$

then the thermodynamic correction factor is

$$\Gamma_i = 1/(1-\theta_i) \tag{4}$$

A combination of eqs (2) and (4) gives

$$D_i = Đ_i/(1-\theta_i) \tag{5}$$

which shows that the Fick diffusivity D_i should increase sharply with as the fractional loading approaches unity; this strong loading dependence is verified by experimental data on diffusion of oxygen and nitrogen in carbon molecular sieve [16] and for diffusion of benzene in silicalite [17]; see Fig. 1.

An important consequence of the non-linearity of the Fick diffusivity is the adsorption and desorption do not proceed at the same rate. During the adsorption process the Fick diffusivity increases with time, i.e. with loading. During the desorption process the Fick diffusivity decreases with time. Desorption proceeds considerably more slowly than adsorption. This asymmetry is illustrated by calculations for diffusion of ethane in 4A zeolite presented in Fig. 2, which were obtained by solving the partial differential equation (1) subject to the following conditions:

$$\text{initial condition}: t = 0; \quad 0 < r < r_c: \quad q_i = q_{i,0} \tag{6}$$

$$\text{boundary (surface) condition}: t > 0; \quad r = r_c: \quad q_i = q_{i,s} \tag{7}$$

where r_c is the radius of the spherical microporous particle. The Maxwell-Stefan diffusivity of ethane is $Đ_1/r_c^2 = 2.45\times10^{-4}\ \mathrm{s}^{-1}$. The method of lines [18] was used to solve the set of equations. The y-axis in Fig. 2 represents the fractional approach to equilibrium, defined as $(\overline{q}_i - q_{i,0})/(q_{i,s} - q_{i,0})$ where $\overline{q}_t$ is the average loading within the particle at any time t, defined by

$$\overline{q}_t = \frac{3}{r_c^3}\int_0^{r_c} q_t r^2 dr \tag{8}$$

As can be seen in Fig. 2, there is excellent agreement between the experiments [19] and our simulations, and the results confirm the asymmetry in adsorption and desorption kinetics.

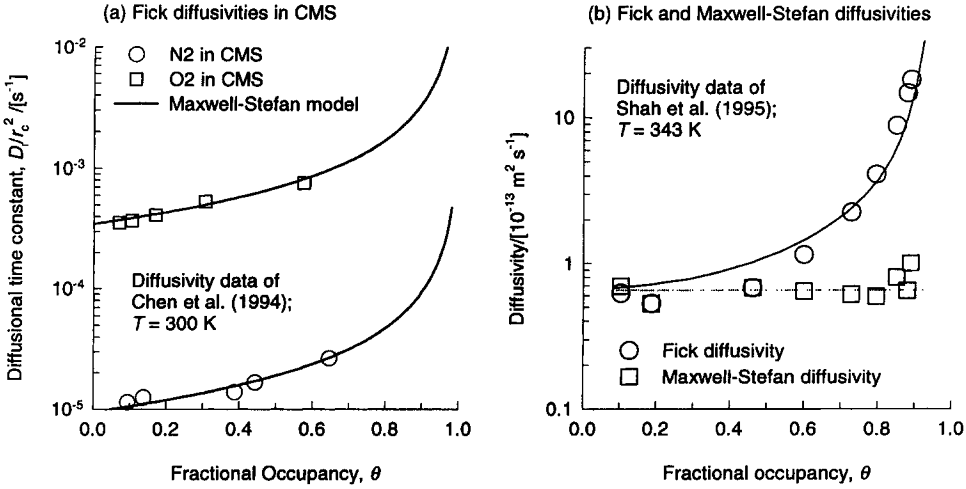

(a) Fick diffusivities in CMS

(b) Fick and Maxwell-Stefan diffusivities

FIG. 1

Dependence of Fick diffusivity on fractional occupancy. (a) Diffusivity of oxygen and nitrogen in CMS [16]. (b) Diffusivity of benzene in silicalite [17].

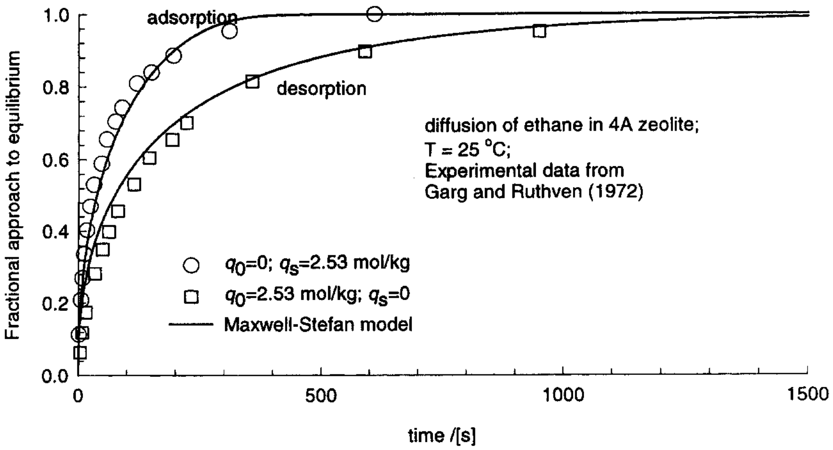

FIG. 2
Adsorption and desorption of ethane in 4A zeolite. Data from Garg and Ruthven [19].

Binary Mixture Diffusion in Spherical Microporous Particle

We now consider diffusion of binary mixture (made up of species 1 and 2) within a spherical particle. The transport process is described again by eq. (1), with index i = 1,2. The D_i in eq. (1) now represent the *effective* Fick diffusivities in the mixture. Using the Maxwell-Stefan diffusion theory developed in our earlier work [4 - 7], these effective diffusivities can be related to the Maxwell-Stefan diffusivities of the pure components in the mixture, $Đ_i$ by:

$$D_i \frac{\partial q_i}{\partial r} = Đ_i \sum_{j=1}^{2} \Gamma_{ij} \frac{\partial q_j}{\partial r}; \quad i=1,2 \tag{9}$$

where Γ_{ij} are the elements of the matrix of thermodynamic correction factors given by [4,5]

$$\Gamma_{ij} \equiv \left(\frac{q_{j,sat}}{q_{i,sat}} \right) \frac{\partial \ln p_i}{\partial \ln q_j}; \quad i,j=1,2 \tag{10}$$

When the binary mixture equilibrium is described by the multicomponent Langmuir isotherm

$$\theta_i = \frac{q_i}{q_{i,sat}} = \frac{b_i p_i}{1 + b_1 p_1 + b_2 p_2}; \quad i=1,2 \tag{11}$$

the following explicit expressions can be derived for the effective diffusivities

$$D_1 = \frac{Đ_1}{(1-\theta_1-\theta_2)} \left((1-\theta_2) + \theta_1 \frac{\partial q_2/\partial r}{\partial q_1/\partial r} \right) \tag{12}$$

$$D_2 = \frac{Đ_2}{(1-\theta_1-\theta_2)} \left((1-\theta_1) + \theta_2 \frac{\partial q_1/\partial r}{\partial q_2/\partial r} \right) \tag{13}$$

There are two important points to note about eqs (12) and (13). Firstly, the effective diffusivities D_i in a binary mixture are strongly dependent on the loadings or occupancies. Secondly, the efffective diffusivity of any component 1 *or* 2 is affected by the gradients in the loadings of components 1 *and* 2. This interdependence of the diffusivities on the loading gradients imparts special features to binary mixture diffusion, especially when the components 1 and 2 have vastly different mobilities.

Let us first consider diffusion of a mixture of oxygen (species 1) and nitrogen (species 2) in a spherical particle of carbon molecular sieve (CMS) at a temperature of 300 K. The Maxwell-Stefan diffusivities of the pure components were determined by Chen et al. [16] as $Đ_1/r_c^2 = 3.478\times10^{-4}$ s^{-1}and $Đ_2/r_c^2 = 9.514\times10^{-6}$ s^{-1}. We note that even the small difference in the kinetic diameters of oxygen and nitrogen leads a significant difference in the Maxwell-Stefan diffusivity values. These values were used in conjunction with eqs (2) and (4) to calculate the Fick diffusivities in the model calculations shown by the continuous lines in Fig. 1 (a). The saturation loadings of oxygen and nitrogen have been determined to be $q_{1,sat}$ = 1.874; $q_{2,sat}$ = 1.469 mol/kg. In one of the experiments reported by Chen et al. [16] (see their Fig. 13), the CMS had initial loadings $q_{1,0} = q_{2,0} = 0$. At time $t = 0$, the outer surface is brought into contact with a binary mixture of oxygen and nitrogen such that the sorption loadings at the surface are $q_{1,s}$ = 0.19635; $q_{2,s}$ = 0.48815 mol/kg. The average uptake by the particle, $\bar{q}_i$, was measured as a function of time. Figure 3(a) shows their experimental data expressed in terms of the fractional approach to equilibrium $(\bar{q}_i - q_{i,0})/(q_{i,s} - q_{i,0})$ as a function of time t. We note clearly that the faster diffusing molecule overshoots its equilibrium value; witness the fractional approach values exceeding unity. Supra-equilibrium loadings are special characteristics of mixture diffusion.

Also shown in Fig. 3 (a) with continuous lines are the simulations of this experiment by solution of the coupled partial differential equations (1), along with eqs (12) and (13) for the effective diffusivity values of components 1 and 2 in the binary mixture. The overshoot of oxygen is also predicted by the Maxwell-Stefan model. It is to be stressed that the binary mixture predictions are on the basis of the pure component Maxwell-Stefan diffusivity values. Also shown with dashed lines are the predictions of the fractional uptake if each component were assumed to diffuse independent of the other. We note that the oxygen uptake profile does not exhibit an overshoot in this case; this is clearly not in conformity with experiment. For nitrogen, both Maxwell-Stefan and independent diffusion models predict uptake profiles that are indistinguishable from each other. For binary diffusion in microporous materials the faster-diffusing species is more significantly affected by "coupling" with the slower-diffusing species.

Let us next consider diffusion of a mixture of methane (species 1) and ethane (species 2) in a spherical particle of 4A zeolite at a temperature of 298 K. Several single component and binary uptake experiments were carried out by Carlson and Dranoff [20]. From their data the Maxwell-Stefan diffusivities can be determined as $Đ_1/r_c^2 = 1.4\times10^{-4}$ s^{-1}and $Đ_2/r_c^2 = 2.2\times10^{-5}$ s^{-1}. The saturation loadings of methane and ethane have been determined to be $q_{1,sat} = 4.245$; $q_{2,sat} = 2.83$ mol/kg. In one of the experiments reported by Carlson and Dranoff [20] (see their Fig. 5), the 4A zeolite had initial loadings $q_{1,0} = q_{2,0} = 0$. At time $t = 0$, the outer surface is brought into contact with a binary mixture of metahne and ethane such that the sorption loadings at the surface are $q_{1,s} = 0.006$; $q_{2,s} = 1.0$ mol/kg. The average uptake by the particle, $\bar{q}_i$ was measured as a function of time. Figure 3(b) shows their experimental data expressed in terms of the fractional approach to equilibrium $(\bar{q}_i - q_{i,0})/(q_{i,s} - q_{i,0})$ as a function of time t. We note clearly that the faster diffusing methane molecule exhibits an overshoot.

Also shown in Fig. 3 (b) with continuous lines are the simulations of the Carlson and Dranoff experiment using eqs (1), (12) and (13). The simulations also confirm the overshoot for the faster-moving methane. Also shown with dashed lines are the predictions of the fractional uptake if each component were assumed to diffuse independent of the other. We note that the methane uptake profile does not exhibit an overshoot in this case; this is clearly not in conformity with experiment. For ethane, both models predictions are indistinguishable from each other.

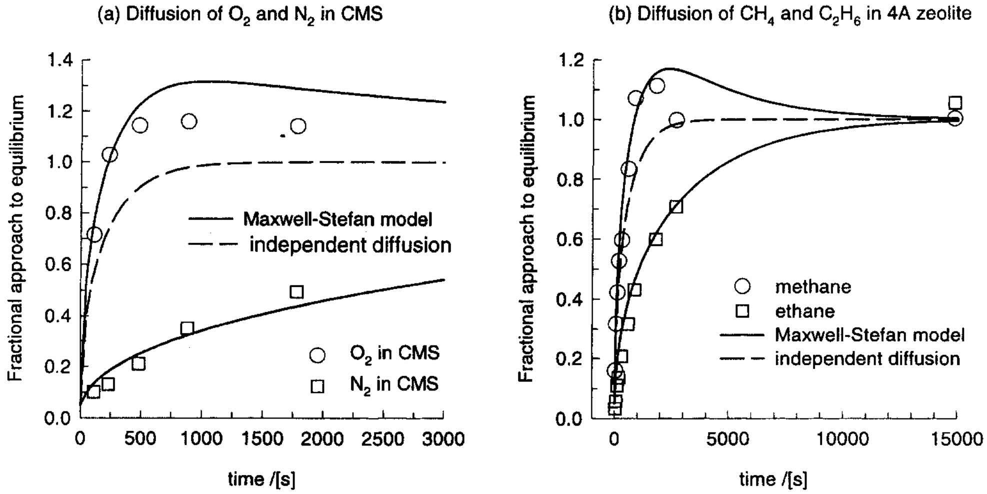

FIG. 3
Uptake of binary mixtures in spherical microporous particle. (a) Diffusion of oxygen and nitrogen in CMS [16]. (b) Diffusion of methane and ethane in 4A zeolite [20].

Co- vs Counter-Diffusion of Binary Mixture Inside Spherical Microporous Particle

Now we demonstrate the differences between co- and counter-diffusion of binary mixtures. Let us first consider co-diffusion of n-heptane (1) and benzene (2) inside a spherical particle of NaX zeolite. Normal heptane being a slender molecule has a mobility 20 times higher than that of benzene, and so we take $Ð_1/Ð_2$ = 20. However, the polarity of benzene is much higher than that of n-heptane: the sorption strengths are in the ratio b_2/b_1 = 8. Simulations of co-diffusion for a surface loading $q_{1,s}$ = 0.2; $q_{2,s}$ = 1.6 mol/kg, starting with a fresh zeolite, i.e. $q_{1,0} = q_{2,0}$ = 0.001 mol/kg, are shown in Fig. 4 (a). The curious maximum in the n-heptane uptake profile is noteworthy and can be explained as follows. Initially, beginning with fresh zeolite crystals, *n*-heptane quickly penetrates the pores of the zeolite occupying the sorption sites because of its higher mobility. The sorption strength of *n*-heptane is however considerably lower than that of benzene and the adsorbed *n*-heptane eventually gets displaced from the sorption sites by benzene and the occupancy of *n*-heptane decreases from its maximum value to reach its final, low, equilibrium value. At equilibrium the pores of the zeolite are occupied predominantly by the more strongly adsorbed benzene. The experimentally measured transient uptake profiles by Kärger and Bülow [21], also shown in Fig. 4 (a), confirm the n-heptane maximum predicted theoretically. Simulations assuming each component diffuses independently of the other do not display a maximum in the uptake of n-heptane.

In Fig. 4 (b) the simulations are repeated for a situation in which the zeolite crystal is loaded with benzene, i.e. i.e. $q_{1,0}$ = 0; $q_{2,0}$ = 1.6 and the surface is maintained at $q_{1,s}$ = 0.2; $q_{2,s}$ = 0 mol/kg. The simulations of the counter-diffusion process shows a completely different uptake profile for n-heptane compared to the co-diffusion case; there is no maximum in the uptake.

Another important feature of binary mixture diffusion is that co- and counter-diffusion are not symmetric in nature.

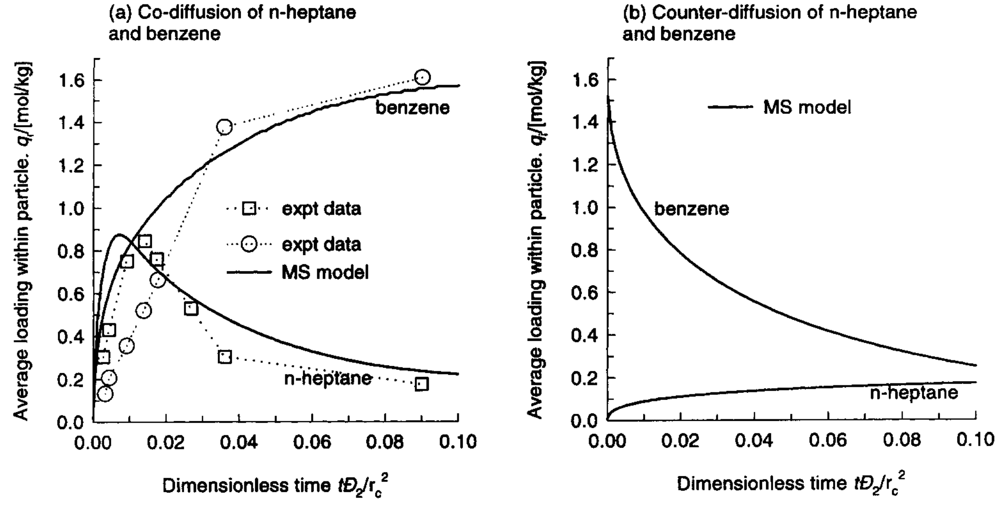

FIG. 4
Co- and counter-diffusion of n-heptane and benzene in NaX zeolite. Data from [21].

Roll-up Phenomena in Packed Bed Adsorber

Industrial sorption separation processes are usually carried out in a packed bed. Adsorption separation processes depend on the preferential adsorption of one component due to either a more favourable equilibrium or faster intra-particle diffusion kinetics. In an equilibrium-driven separation process, the phenomenon of "roll-up" is usually observed in the breakthrough curves [1, 22]. The more strongly adsorbed component displaces the weaker component, leading to a rise in the effluent concentration of the less strongly adsorbed component above its inlet value.

We now consider the breakthrough behaviour of a mixture where the roll-up phenomon occurs but this is caused not by differences in the sorption strengths but by differences in intra-particle diffusivities. We shall illustrate this with the example of air separation using the data provide by Farooq and Ruthven [22]. We simulated the breakthrough curves for oxygen (1) and nitrogen (2) on Bergbau-Forschung carbon molecular sieve. The feed composition is O_2: 21%; N_2: 79%. Other parameters in the simulation are as follows. Packed bed length 0.7 m; column diameter = 0.035 m; inlet superficial gas velocity = 0.0152 m/s; bed porosity $\varepsilon = 0.4$; radius of particle, r_c = 0.005 m; temperature, assumed isothermal, T = 294 K; pressure, assumed constant, p = 100 kPa. The Maxwell-Stefan diffusivities: $Đ_1/r_c^2 = 2.7\times10^{-3}\ \mathrm{s}^{-1}$; $Đ_2/r_c^2 = 5.9\times10^{-5}\ \mathrm{s}^{-1}$. The Langmuir parameters are b_1 = 1.43×10^{-6} Pa^{-1}; b_2 = 1.38×10^{-6} Pa^{-1}. The saturation loadings are $q_{1,\mathrm{sat}} = q_{2,\mathrm{sat}}$ =1.47 mol/kg; particle density, ρ =1800 kg/m^3.

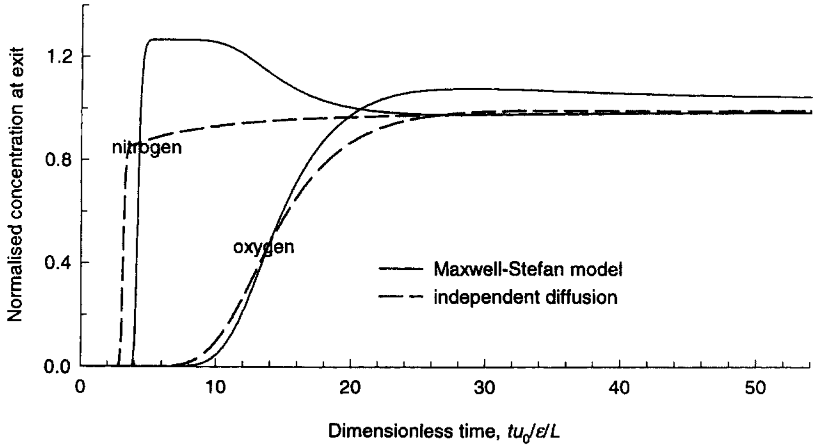

FIG. 5
Breakthrough of oxygen and nitrogen through a packed bed adsorber of microporous particles of CMS. The process data are from Farooq and Ruthven [22].

The breakthrough curves are shown in Fig. 5; the effluent gas phase concentration is plotted on the y-axis and this is normalized with respect to the inlet concentration c_0. A roll-up phenomenon is observed for the species nitrogen which has a lower diffusivity *inside* the CMS particles. Consequently, the concentration of nitrogen in the gas phase surrounding the particle can increase above its initial concentration, c_0, leading to roll-up phenomenon. Also shown with dashed lines are the breakthrough calculated if each component were to diffuse independently of the other; no roll-up is observed with the independent diffusion model.

As pointed out by Ruthven et al. [2], accurate modelling of the diffusion process is essential for successful commercialisation of the pressure swing adsorption technology for air separation.

Conclusions

The Maxwell-Stefan formulation for micropore diffusion developed by us earlier [4 – 7] has been used to highlight some peculiar transport characteristics inside a spherical particle and in a packed bed adsorber. The following major observations and conclusions can be drawn.

- For single component diffusion, *ad*sorption and *de*sorption processes are asymmetric; desorption proceeds significantly more slowly.
- For binary mixture uptake into a microporous particle, the faster-diffusing species can overshoot its equilibrium value; this overshoot is caused by coupling between the diffusing species. A model in which each component is assumed to diffuse independently, does not predict an overshoot.
- The predictions of the Maxwell-Stefan diffusion model are in good qualitative and quantitative agreement with published experimental data for intra-particle diffusion.
- Co- and counter-diffusion of binary mixtures are asymmetric phenomena.
- The breakthrough behaviour in a packed an adsorber packed with microporous particles exhibits roll-up phenomenon. This roll-up is caused by differences in the Maxwell-Stefan diffusivities inside the particle. A proper description of such effects is essential in the design of pressure swing adsorption separation processes.

Acknowledgment

RK acknowledges a grant *Programmasubsidie* from the Netherlands Organisation for Scientific Research (NWO) for development of novel concepts in reactive separations technology.

References

1. J. Kärger and D.M. Ruthven, *Diffusion in Zeolites*, John Wiley, New York, 1992.

2. D.M. Ruthven, S. Farooq and K.S. Knaebel, *Pressure Swing Adsorption*, VCH Publishers, New York, 1994.

3. R. Krishna, B. Smit Vlugt, T.J.H., *J.Phys.Chem. A*, **102**, 7727 (1998).

4. R. Krishna and J.A. Wesselingh, *Chem. Eng. Sci.*, **52,** 861 (1997).

5. F. Kapteijn, J.A. Moulijn and R. Krishna, *Chem. Eng. Sci.*, **55**, 2923 (2000).

6. R. Krishna, T.J.H. Vlugt and B. Smit, *Chem. Eng. Sci.*, **54**, 1751 (1999).

7. R. Krishna and D. Paschek, *Ind.Eng.Chem. Research*, **39**, 2618 (2000).

8. C. Saravanan and S.M. Auerbach, *J. Chem. Phys.*, **110**, 11000 (1999).

9. D. Paschek and R. Krishna, *Physical Chemistry Chemical Physics*, **2**, 2389 (2000).

10. R.Q. Snurr and J. Kärger, *J. Phys. Chem. B.*, **101,** 6469 (1997).

11. S. Jost, N.K. Bär, S. Fritzsche, R. Haberlandt and J. Kärger, *J.Phys.Chem. B*, **102**, 6375 (1998).

12. D. Schuring, A.P.J. Jansen and R.A. van Santen, *J.Phys.Chem. B*, **104,** 941 (2000).

13. L.N. Gergidis and D.N. Theodorou, *J. Phys. Chem. B.*, **103,** 3380 (1999).

14. L.N. Gergidis, D.N. Theodorou and H. Jobic, *J. Phys. Chem. B.*, **104,** 5541 (2000).

15. C.C. Ni and J.Y. San, *Int. J. Heat. Mass Transfer*, **43,** 2129 (2000).

16. Y.D. Chen, R.T. Yang and P. Uawithya, *A.I.Ch.E.J.*, **40,** 577 (1994).

17. D.B. Shah, C.J. Guo and D.T. Hayhurst, *J. Chem.Soc. Farad. Trans.*, **91,** 1143 (1995).

18. W.E. Schiesser, *The numerical method of lines: Integration of partial differential equations*, Academic Press, San Diego, 1991

19. D.R. Garg and D.M. Ruthven, *Chem. Eng. Sci.*, **27,** 417 (1972).

20. N.W. Carlson and J.S. Dranoff, In Fundamentals of Adsorption, Edited by A.I. Liapis, American Institute of Chemical Engineers, New York, 1981.

21. J. Kärger and M. Bülow, *Chem. Eng. Sci.* **30**, 893 (1975).

22. S. Farooq and D.M. Ruthven, *A.I.Ch.E.J.*, **37,** 299 (1991).

Received September 8, 2000